 DOI 10.1515/ract-2014-2163 — Radiochim. Acta 2014; 102(7): 629–643

Trevor Zimmerman, Mavrik Zavarin, and Brian A. Powell*

Influence of humic acid on plutonium sorption to gibbsite: Determination of Pu-humic acid complexation constants and ternary sorption studies

Abstract: In this work stability constants describing Pu(IV), Th(IV), and Np(V) binding to Leonardite humic acid (HA) were determined using a discrete pK_a model. A hybrid ultra-filtration/equilibrium dialysis, ligand exchange technique was used to generate the partitioning data. Ethylenediaminetetraacetic acid (EDTA) was used as a reference ligand to allow the aqueous chemistry of the Pu(IV)-HA system to be examined over a range of pH values, while minimizing the possibility of precipitation of Pu(IV). The conditional stability constant for Pu(IV) complexation with HA determined as part of this work is $\log \beta_{112} = 6.76 \pm 0.14$ based on the equation: $Pu^{4+} + HL3 + 2H_2O \leftrightarrow Pu(OH)_2L3^+ + 3H^+$ where HA is represented by HL3 (a binding site on the HA with a pK_a value of 7). This value is three orders of magnitude higher than the Th(IV)-HA constant and between six and eight orders of magnitude higher than the Np(V)-HA complex. The magnitude of the stability constants and the general trend of increasing complexation strength with increasing pH is consistent with previous observations.

The Pu(IV)-HA stability constants were used to model sorption of Pu(IV) to gibbsite in the presence of HA. Assuming only aqueous Pu-HA complexes and AlOH-Pu surface complexes, the model was unable to predict the observed data which exhibited greater sorption at pH 4 relative to pH 6; a phenomenon which does not occur in the absence of HA. Therefore, this study demonstrates that ternary Pu-HA-gibbsite complexes may form under low pH conditions and exhibit greater sorption than that observed in the absence of HA. Although the presence of HA may increase the solubility/aqueous concentrations of Pu in the absence of a solid phase, formation of ternary complexes may indeed retard the subsurface migration of Pu. The corollary to this finding is that increased mobility may occur if the ternary surface complex forms on a mobile colloid rather than part of the subsurface matrix

Keywords: Plutonium, Humic acid, Sorption, Ternary complex, Gibbsite.

***Corresponding Author: Brian A. Powell,** Environmental Engineering and Earth Sciences, Clemson University, Anderson, SC 29625, USA, e-mail: bpowell@clemson.edu

Trevor Zimmerman: Environmental Engineering and Earth Sciences, Clemson University, Anderson, SC 29625, USA

Mavrik Zavarin: Glenn T. Seaborg Institute, Physical and Life Sciences Directorate, Lawrence Livermore National Laboratory, Livermore, CA 94551, USA

1 Introduction

This work examined the interaction between Pu, Np, and Th and humic acid (HA) (a refractory component of natural organic matter (NOM)) in the context of these various processes. Specifically, the conditional stability constants for the actinide–HA complexes were determined and the influence of HA on Pu sorption was explored. An understanding of the chemical, physical, and biological processes controlling the mobility of actinides in the environment is imperative for protecting human and environmental health. Processes which play a critical role in actinide transport, include oxidation/reduction (redox), complexation, sorption/desorption, and solubility. Aqueous complexation with NOM will effect all of these processes.

NOM is ubiquitous in soils and waters in the environment. Commonly found coating the surface of inorganic material, NOM can change surface characteristics and affect mineral colloid stability and mobility [1]. The presence of dissolved NOM has been shown to result in the formation of stable Pu-NOM solution complexes and the reduction of Pu(V) to Pu(IV) [2–7]. A few studies suggest that the distribution coefficients for Pu sorption to sediments and aquifer materials decrease in the presence of NOM [3, 8–12]. However, other researchers have shown that sorption of Pu in systems containing organic ligands may be enhanced under low pH conditions and decreased under high pH conditions [9, 12, 13]. In addition,

recent literature suggests that the sorption of Pu(V) onto silica particles can be enhanced in the presence of colloidal organic matter such as extracellular polymeric substances [6]. Currently, little information is available regarding the effects of organic surface coatings on the kinetics of Pu sorption/desorption reactions on mineral colloids. Sorption of NOM to mineral colloids is relatively slow when compared to Pu sorption. The equilibria and kinetics of Pu behavior in ternary Pu-NOM-mineral colloid systems are likely to be influenced by: (a) the order in which Pu and NOM are deposited on the particle surface; (b) Pu solution concentrations and the concentration ratios of Pu to organic ligands and to mineral surface sites; and (c) physical and chemical NOM characteristics, such as molecular size and structure.

Although both mineral colloids and NOM in solution can facilitate Pu transport, the required conditions and limitations for these two modes of transport may be substantially different. Hence, it is necessary to understand the partitioning of Pu between these mobile phases as well as the potential for formation of ternary suface complexes. For example, if NOM enhances and stabilizes Pu sorption onto mineral colloids, this will facilitate the transport of Pu as a ternary Pu-NOM-mineral colloid complex. On the other hand, if NOM decreases Pu sorption, Pu could be primarily mobile as Pu-NOM solution complexes

A detailed study of Pu-NOM interactions must cover a wide pH range. However those studies are difficult due to the strong hydrolysis of Pu(IV) and precipitation of PuO_2(s). Previous studies have attempted to mitigate precipitation of the actinide of interest by working at low pH. Banik *et al.* [3] examined the ternary Pu-HA-kaolinite system and also conducted aqueous Pu-HA complexation studies with commercially available Aldrich HA (Sigma-Aldrich Company). Using ultra-filtration, Banik *et al.* [3] and Buda *et al.*, [9] reported stability constants ($\log \beta$) for Pu(IV)-HA ranging from 6.4 to 8.4 over the pH range: 1.8–3. Without a competing complexant as done in this current work, these studies are limited to a low pH range due to concerns of precipitation of Pu(IV)-(hydr)oxide solids. Conversely, at low pH values there is concern over precipitation of HA (and subsequent co-precipitation of Pu).

Previous studies by Banik *et al.* [3] and Buda *et al.* [9] determined Pu(IV)-HA stability constants using a charge neutralization model in which the stability constant is normalized to a loading capacity (LC) term [14]. This is a simple yet powerful model which can describe metal-HA binding across a wide range of experimental conditions. In this paper a slightly different discrete ligand model was utilized to describe proton-binding and actinide binding with HA. This technique is similar to that used by Westall *et al.* [15] to study Co complexation by Leonardite HA as well as Pu complexation with a variety of ligands [16, 17]. This approach assumes that the HA can be represented by a discrete number of monoprotic acid sites with a fixed pK_a spectrum (e.g., $pK_a = 3$, 5, 7, and 9 in this work). From acid-base titration data, the total number of binding sites at each pK_a value can then be determined. This approach simplifies the complexity of natural organic matter such that it is represented by a distribution of sites. This approach is not intended to provide a true molecular understanding of the complexation sites, nor does it consider electrostatic interactions with charged sites. Rather this simplified approach is intended to provide a quantitative prediction of the binding of plutonium to the humic acid which essentially captures only the influence of the Pu : HA molar ratio and the general influence of pH on ligand binding. This model was selected over the charge neutralization model as it can be seamlessly integrated into existing aqueous speciation modeling programs. While the charge neutralization model also presents a simplified model, the specific loading capacity term (LC) must still be determined for each NOM-metal complex. A recent review of radionuclide-HA interactions by Bryan *et al.*, [18] noted that despite advances in computing, radiological performance assessment models still typically rely on simple chemical models and the ability for full and seamless integration into existing aqueous thermochemical models was determined to be a high priority. Thus the even simpler discrete pK_a model in which the HA is modeled as a series of monoprotic acids with discrete pK_a values was selected. For comparative purposes with Pu(IV) measurements, stability constants for Np(V) and Th(IV) were also determined.

2 Materials and methods

2.1 Humic acid preparation

Unless stated otherwise, all chemicals used in this study were ACS reagent grade or higher. Water for all experiments was supplied from a Millipore Super-Q water system (MQ-water) and had a resistivity of greater than 18.2 M Ω cm. Labware was cleaned by sequential base (0.1 M NaOH) and acid baths (0.1 M HCl), then rinsed at least five times with MQ-water and dried. Leonardite HA, available as a dried solid was purchased from the International Humic Substances Society (IHSS). The HA was rehydrated and converted to the fully-protonated form by dissolving an appropriate quantity of HA in 0.1 M NaCl and then increasing the solution pH to approximately 9. After

the HA was fully dissolved (approximately 24 h) the pH was decreased to approximately 5. The HA was then dialyzed using 1000 molecular weight cut-off (MWCO) dialysis tubing *versus* 0.1 M NaCl for one week with daily renewal of the dialysis solution. The dialyzed HA stock solution concentration was then quantified using a Shimadzu TOC-V CSH total organic carbon (TOC) analyzer and stored in a cleaned amber glass bottle at 4 °C until needed.

2.2 Humic acid titration

All titrations were conducted using a Metrohm 836 Titrino titrator under an inert, Ar(g), atmosphere at 25 °C. Before introduction to the headspace of the titration vessel, the Ar(g) was passed through NaOH to remove CO_2(g) and "wet" the gas. The temperature was controlled using a jacketed titration vessel connected to a constant temperature water bath and the temperature and pH were continuously monitored using a Metrohm Pt 1000 electrode and the system pH was continuously monitored using a Thermo Fisher Orion Ross Sure-Flow combination electrode. The system was cycled a total of five times using the following criteria between acid/base additions. After an initial addition of 0.1 mL 0.1 N HCl to achieve a desirable starting point (pH ≈ 3.5), the titrations were carried out as follows. Forward (base) titrations were performed using 0.025 mL additions of 0.1 N NaOH and an electrode stability criterion between additions of 0.1 mV min^{-1}. Back (acid) titrations were conducted using 0.025 mL additions of 0.1 N HCl. The stability criterion for each back titration was varied for each cycle as: cycles 1 and 2, 30 s before next addition; cycle 3, 10 min before next addition; cycle 4, 1 h before next addition; and cycle 5, 2 h before next addition. These parameters were determined during preliminary titrations in order to minimize hysteresis during forward and reverse titration steps and also limit drift in the pH electrode calibration. The initial HA concentration at the start of the titration was 50 mg C/L as determined using TOC analysis.

Using the known volumes and concentrations of acid and base added, the total concentration of H^+ (T_H^{EXP}) in the system can be determined using Eq. (1) after Westall *et al.* [15]:

$$T_H^{EXP} = C_a - C_b + T_H^o = \Delta T_H + T_H^o \quad (1)$$

where C_a and C_b represent the total concentrations of strong acid and base added to the system during the course of a titration, and T_H^o represents the concentration of acid or base initially present (e.g., added during HA rehydration). While Ca and Cb are known, the concentration of T_H^o (mol/L) was determined by modeling the titration data using FITEQL. A discrete pK_a approach was assumed to model the data using four sites with pK_a values of 3, 5, 7, and 9. The consumption of acid and base by water was accounted for by including the dissociation constant of water (K_w).

2.3 Actinide – humic acid complexation studies

The partitioning of Pu between HA and EDTA was examined using a combined ultrafiltration and competitive ligand exchange technique. This technique was used because it combines the positive aspects of ultrafiltration previously used for Pu complexation studies (Banik *et al.*, 2007) with competitive ligand approaches, which can maintain Pu(IV) as the dominant oxidation state and also prevent precipitation of sparsely soluble PuO_2(s). The ^{242}Pu stock solution was prepared by dissolving 1 mg of $Pu(NO_3)_4$ (New Brunswick Laboratory, CRM 130) in 8 M HNO_3. Solvent extraction was used to verify Pu(IV) as the dominant oxidation state in the working solution. The final concentration was determined using inductively coupled plasma mass spectrometry (ICP-MS) as described below.

A ^{237}Np stock solution from Isotope Products (Valencia, CA) was purified by ion exchange and diluted to 4.2×10^{-6} M in 0.1 M HNO_3 for use in this work. The oxidation state of Np was not verified, but should be Np(V) based on the separation scheme used and the oxic conditions of these experiments. A 1000 μg/mL ^{232}Th (4.3×10^{-3} M) calibration standard in 2% HNO_3 was purchased from High Purity Standards (Charleston, SC) and used as the ^{232}Th(IV) stock solution.

Determination of ^{242}Pu, ^{237}Np, and ^{232}Th concentrations was performed on a Thermo Scientific X Series II ICP-MS. NIST standard reference materials (^{242}Pu SRM 4334I and ^{237}Np SRM 4341) and the ^{232}Th stock solution from High Purity Standards were used to prepare calibration standards for ICP-MS analysis. Typical ICP-MS analysis is performed in a 2% HNO_3 solution. However, under these conditions the HA and EDTA form an insoluble precipitate thus making 2% HNO_3 an unacceptable matrix for these analyses. Therefore, all samples were prepared in 0.01 M Na_4EDTA and analyzed using matrix matched standards. The presence of EDTA was required to overcome the propensity for actinides to hydrolyze and precipitate at high pH. ^{238}U and ^{232}Th were used as internal standards during analysis of samples containing ^{242}Pu and ^{237}Np. In Th-HA complexation studies, ^{208}Pb was used in place

of ^{232}Th as an internal standard. The resulting calibration curves yielded detection limits on the order of 10^{-14} M for ^{232}Th, ^{242}Pu and ^{237}Np based on the intercept of calibration curves. This was consistent with detection limits achieved using 2% HNO_3.

Complexation studies were conducted with 4.3×10^{-8} M (10 ppb) and 2.6×10^{-7} M (63 ppb) ^{242}Pu, 4.3×10^{-8} M (10 ppb) and 2.6×10^{-8} M (5 ppb) ^{237}Np, and 4.9×10^{-8} M (11 ppb) ^{232}Th. The solutions in Th(IV) and Pu(IV) complexation studies contained fixed concentrations of 1×10^{-5} M EDTA, 10 mg C/L HA, and 0.1 M NaCl, regardless of the actinide concentration. Due to the relatively high solubility of Np(V), a competing/solubilizing ligand was not necessary, eliminating the need for EDTA. The pH of the samples was adjusted using a minimum of 0.1 N HCl or 0.1 N NaOH to produce a distribution of samples over the pH range: 4–6.5. Samples were prepared in 50 mL polypropylene vials and mixed on an orbital shaker at 25 °C. Homogenous aliquots were removed after 24 h, 1 week, and 2 weeks for an experiment with 2.6×10^{-7} M ^{242}Pu. There was no observable change in the distribution after 1 week, so a single 1.5-week sampling event was used in all other experiments.

Preliminary experiments showed that Millipore 3 kDa Amicon® Ultra-4 centrifugal filters achieved complete removal of HA, while allowing greater than 99% recovery of the Pu-EDTA complex. These filters employ regenerated cellulose membranes which were compatible with UV-Vis and TOC analysis of the filtrate in HA exclusion experiments. Filters were pre-rinsed with approximately 2 mL 0.01 M EDTA (Th and Pu studies) or 2 mL of 0.1 M NaCl (Np studies) prior to filtration. A 4 mL aliquot of the solution was then transferred to the pre-rinsed centrifugal filter and centrifuged at 3000 rotations min^{-1} using a Beckman GS-6 centrifuge. Approximately 2 mL was passed through the filter as a further pre-equilibration step and discarded. Then the final 2 mL was collected for analysis and an aliquot was diluted to 10 mL in 0.01 M EDTA for final ICPMS analysis.

The fraction of each actinide bound to HA was determined using a competitive ligand approach described by Van Loon *et al.*, [19]. The actinide may be present as a free or hydrolyzed ion (An), a HA complex (AnHA), or an EDTA complex (AnL_n). Since the ligands (HA and EDTA) were present in excess relative to the actinide, the assumption can be made that the actinide was only present as an An-HA or An-EDTA complex. This was confirmed for Pu(IV) and Th(IV) using thermochemical modeling utilizing the constants provided in Appendix A. It was also verified that Np(V) was only present as the free NpO_2^+ ion across the pH range examined in this work. Therefore the mass balance expression of the actinide in solution (An = Th, Pu, or Np; L = EDTA) becomes:

$$[An]_{total} = [AnHA] + [AnL_n] \quad (2)$$

Since the filtration step removed HA and An-HA complexes, the concentration of AnL_n is equal to the concentration of actinide in the filtrate:

$$[An]_{filtrate} = [AnL_n] \quad (3)$$

In the case of Np(V) where no EDTA was added, the concentration in the filtrate is only the concentration of the free or hydrolyzed ion; essentially replacing $[AnL_n]$ in Eq. (2) and (3) with $[Np]_{filtrate}$ which is the concentration of Np in the filtrate.

$$[NpHA] = [Np]_{total} - [Np]_{filtrate} \quad (4)$$

Therefore, the concentration of the actinide bound to HA can be determined subtracting the concentration of actinide in the filtrate from the total concentration.

2.4 Binary sorption studies

As a baseline of comparison with ternary Pu-HA-mineral systems, sorption of Pu(IV) and Pu(V) to gibbsite as a function of pH was examined. Gibbsite (Ward's Scientific) was purified by suspending 10 g of the mineral in 180 mL 0.1 M NaOH. This suspension was mixed for one hour, and then centrifuged for 20 min at 8000 rotations min^{-1} using a Sorvall Evolution RC centrifuge with a SLA-1500 Superlite fixed-angle rotor. This centrifugation procedure was calculated to leave particles less than 100 nm in the supernatant. The NaOH supernatant was then decanted and the solution was replaced with 0.1 M HCl, mixed for 1 h, and then centrifuged again using the parameters outlined above. The HCl was decanted and replaced with ultra-pure MQ-water. This suspension was mixed for approximately 1 h, centrifuged, and the aqueous phase was decanted. The solids were washed with MQ-water an additional four times using the procedure described above. The final wet solids were transferred to a glass petri dish and dried in an oven at 40 °C. After drying, the solids were lightly ground with a mortar and pestle to break up large aggregates and then stored in a glass vial.

Sorption from pH 3 to 9 was examined by amending 10 g/L gibbsite suspensions in 0.1 M NaCl with ^{238}Pu(IV) or ^{238}Pu(V) at total concentrations of 1.3×10^{-10} M Pu. Trace level concentrations of Pu were used in these experiments to minimize the possibility of precipitation of a discrete Pu-oxide phase since no complexing ligands were

used in these studies. No effort was made to prevent CO_2(g) intrusion into the samples.

A 1.2×10^{-6} M ^{238}Pu stock solution was purchased from Isotope products (Valencia, CA). Pu(IV) working solutions were prepared by transferring a small aliquot of the ^{238}Pu stock solution to a Teflon vial and heating the solution until incipient dryness was reached. Then 0.1 M HCl was added to the vial (less than 1 mL) along with 10 μL of 0.1 M $NaNO_2$. To prevent precipitation of $Pu(OH)_4$(s) and to keep Pu in the tetravalent oxidation state, the solution was maintained at pH < 1. Therefore, the total volume was kept low to minimize the need for adjustment of sample pH values following the addition of the Pu(IV) working solution spike.

To prepare a Pu(V) working solution, a small aliquot of the 1.2 μM ^{238}Pu stock solution was evaporated to dryness then dissolved in 0.5 mL 1.0 M HCl/0.2 mM $KMnO_4$ in a plastic vial. The vial was wrapped in Al foil and left for 8 h to oxidize all Pu to Pu(VI). The solution was diluted approximately 200x with 5 mM NaCl to the pH range 2–3. A 10 μL aliquot of 0.01 M $MnCl_2$ was added to precipitate any remaining permanganate. Note, the pH must be kept low (< 3) during this step to avoid co-precipitating Pu. The solution was then passed through a 100 nm nylon syringe filter into a Teflon bottle, adjusted to pH 3 using NaOH and left for 5 d to allow autoreduction of Pu(VI) to Pu(V). The oxidation state purity of the ^{238}Pu(IV) and ^{238}Pu(V) working solution remained stable over the course of the experiments.

After addition of either the Pu(IV) or Pu(V) working solution, the suspensions were adjusted to the desired pH with minimal volumes of either 0.1 M HCl or NaOH then placed on an end over end tumbler. Due to the need to add the Pu(IV) as a small aliquot of an acidic working solution, the pH of Pu(IV) samples was immediately adjusted after addition of the spike to minimize the amount of time the suspension remains at a low pH. Homogenous suspensions were removed after 24 h, 3 d, and 7 d and centrifuged for 20 min at 8000 rotations min^{-1} using an Allegra X-22R centrifuge and a F2402 rotor. Under these conditions, it is estimated that particles less than 100 nm remain in the supernatant which should remove all gibbsite. A 1.0 mL aliquot of the supernatant was removed and mixed with 6 mL HiSafe 3 scintillation cocktail for counting on a Hidex 300 SL liquid scintillation counter. The fraction of Pu sorbed was calculated based on the difference between the initial concentration of Pu and the concentration of Pu in the supernatant.

2.5 Ternary sorption

The influence of HA on Pu sorption to gibbsite was examined using pH 4 and 6 sorption isotherms. A ^{242}Pu-HA stock solution was prepared by heating 0.5 mL of a ^{242}Pu stock solution to dryness a 30 mL Teflon vessel the redissolving in 20 mL of a 10 mg C/L HA solution. The resulting solution was mixed well using careful agitation, and then adjusted to pH 5. The ^{242}Pu concentration in this Pu-HA stock solution was confirmed to be 3.39×10^{-6} M using both ICP-MS and Liquid Scintillation Counting (LSC) on a Hidex 300 SL liquid scintillation counter. LSC measurements were corrected for trace levels of other Pu isotopes present in NBL CRM 130.

Appropriate quantities of gibbsite, HA, and 0.1 M NaCl were added to cleaned 15 mL polypropylene vials to yield 20 samples, each containing 12 mL total volume, with 10 g/L gibbsite, 10 mg C/L HA, and 0.1 M NaCl. Ten of these suspensions were adjusted to pH 4 and the remaining ten samples were adjusted to pH 6 using either 0.1 N HCl or 0.1 N NaOH. After pH adjustments, the gibbsite-HA suspensions were allowed to equilibrate for 24 h on an orbital shaker at 25 °C in the absence of light. An appropriate volume of Pu-HA working solution was then spiked into the gibbsite-HA solutions described above, to yield duplicate samples (at both pH 4 and 6) containing 4.1×10^{-9} to 8.3×10^{-8} M ^{242}Pu. These solutions were then re-adjusted to the appropriate pH as described above, and placed back on the orbital shaker at 25 °C in the absence of light. Homogenous 1.5 mL aliquots were removed from each suspension after 24 h and 7 d. Aliquots were centrifuged at 8000 rpm for 20 min (i.e. calculated to leave particles less than 100 nm in the supernatant). After centrifugation, 1.0 mL of the supernatant was extracted and diluted to 10 mL with 0.01 M EDTA. The concentration of ^{242}Pu in each sample was determined using ICP-MS as described previously.

The final sampling event (after 2 weeks) used a modified sampling procedure. This was done to examine what influence, if any, HA colloids played in the system. It was theorized that HA could aggregate sufficiently to be removed from solution using the centrifugation procedure described above, thereby artificially enhancing the concentration of Pu associated with the "solid phase". The centrifugation parameters were modified to allow the system to be fractionated into < 1500 nm, < 100 nm, and < 3 kDa (nominally considered to be 1–5 nm) size fractions. Solutions were centrifuged for 5 min at 1000 rotations min^{-1} using a C1015 rotor on the Allegra X-22R centrifuge. This step served as a prefiltration step, and was designed to leave particles smaller

than 1500 nm in the aqueous phase. Homogenous 1.0 mL aliquots were then removed and diluted with 9 mL 0.01 M EDTA for quantification of Pu using ICP-MS. The remaining sample was then centrifuged for an additional 20 min at 8000 rpm. From this, a 1.0 mL aliquot of the supernatant was removed and prepared for quantification using the ICP-MS as described above. Finally, an additional 2.0 mL of the supernatant was removed from each centrifuged sample and passed through a 3 kDa Amicon ultra-4 centrifugal filter. Approximately 0.5 mL of the solution was used to pre-equilibrate each filter. The filtrate was then discarded and filtration resumed. Approximately 1.0 mL of the filtrate was collected and prepared for quantification of the ^{242}Pu concentration using ICP-MS.

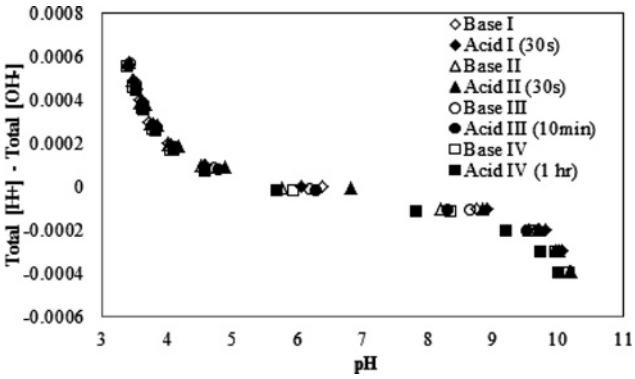


Fig. 1: HA titration data showing five acid-base titration cycles. All base titrations were performed with 0.1 mV min^{-1} as a fixed criteria for electrode stability prior to adding the next aliquot. All acid titrations were performed using a fixed time delay between each aliquot addition as noted in the legend parentheses. Systems parameters: HA concentration: 50 mg C/L, I = 0.1 M NaCl.

3 Results and discussion

3.1 Proton binding modeling

The HA titration data are shown in Figure 1. The titration curves generally follow the same shape although the acid titration curves appear to show some differences which are likely due to the differing equilibration times. Using an electrode stability criteria of 0.1 mV min^{-1} for the acid titrations curves generally resulted in a large amount of hysteresis in the curves. It is hypothesized that during acid titrations where HCl is being added, the kinetics of H^+ displacement of Na^+ from available sites causes the observed differences in titrations at various times. Generally, as the equilibration time for the acid titrations increases, there is greater agreement with the base titrations.

The titration data were fit using a 4-site discrete proton binding model with pK_a values of 3, 5, 7, and 9 (referred to herein as HL1, HL2, HL3, and HL4, respectively). Similar discrete site approaches have been effectively used to quantify metal-HA binding [15–17, 20]. These models attempt to reduce the complexity of HA into a simple binding model that can be easily incorporated into chemical speciation modeling program at the expense of neglecting specific metal-NOM interactions. The data from acid and base titrations IV (Table 1) exhibited the least amount of hysteresis and the pH electrode stability criteria was met during the titration. Therefore the base IV titration curve was selected for the site concentration determination and the model yields excellent agreement with the titration data (Figure 2). Due to the observed apparent hysteresis in the above titrations, there is valid concern that the total number of available sites may be sensitive to specific experimental conditions. Therefore, each of the acid titration curves for each pK_a value were modeled and the calculated site concentrations are also listed in Table 1. There is relatively little variation in the total site concentrations for the overall HA for each site. Therefore, it does not appear that the hysteresis frequently observed in HA titrations will

Table 1: Site concentrations determined from acid-base titrations of HA.

		Site conc. (mol/mg C)				
Titration	Time between additions	HL1	HL2	HL3	HL4	Total binding site conc. (molesites/mg C)
Base (IV)	0.1 mV min^{-1} stability	4.19×10^{-6}	2.06×10^{-6}	1.59×10^{-6}	1.53×10^{-6}	9.37×10^{-6}
Acid (I)	30 s	6.24×10^{-6}	1.98×10^{-6}	1.29×10^{-6}	8.72×10^{-7}	1.04×10^{-5}
Acid (II)	30 s	6.10×10^{-6}	1.98×10^{-6}	1.50×10^{-6}	1.96×10^{-6}	1.16×10^{-5}
Acid (III)	10 min	4.21×10^{-6}	2.25×10^{-6}	2.00×10^{-6}	1.39×10^{-6}	9.86×10^{-6}
Acid (IV)	1 h	6.05×10^{-6}	2.38×10^{-6}	1.57×10^{-6}	2.77×10^{-6}	1.28×10^{-5}
Acid (V)	2 h	3.68×10^{-6}	2.81×10^{-6}	1.93×10^{-6}	1.09×10^{-6}	9.51×10^{-6}

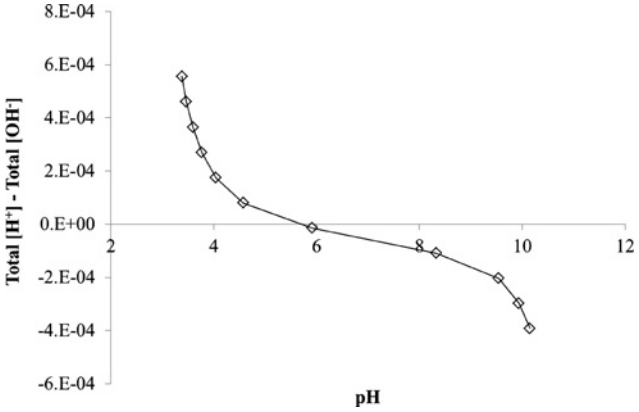


Fig. 2: HA base (IV) titration data with model fit. Model fit generated using FITEQL assuming a 4-site discrete pKa model with values of 3, 5, 7, and 9. Total sites are listed in Table 1.

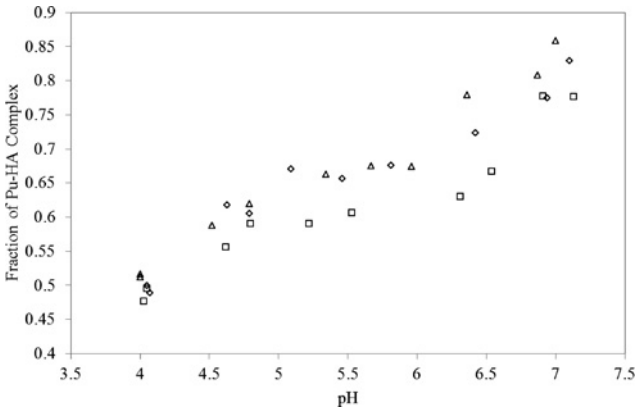


Fig. 3: Pu fraction bound to HA *versus* pH as a function of time. Systems parameters: 2.6×10^{-7} M ^{242}Pu, 0.1 M NaCl, 10 mg C/L HA. Squares 1 day, diamonds, 7 d, and triangles 14 d.

have a significant impact on the overall stability constants determined from this work.

Westall *et al.* [15], using a discrete pK_a spectrum of 4, 6, 8, and 10, reported a total proton-binding site concentration of 1.01×10^{-5} (mol/mg C) for Leonardite HA. This value corresponds very well with the total binding site concentrations shown in Table 1 and the overall average and standard deviation of $1.06 \pm 0.13 \times 10^{-5}$ (mol/mg C) from all curves.

3.2 Actinide – HA complexation and modeling studies

A preliminary experiment using 2.60×10^{-7} M Pu, 10 mg C/L HA, and 1×10^{-5} M EDTA was used to determine the optimal equilibration time. The fraction of Pu bound to HA as a function of time and pH is shown in Figure 3. These data indicate that there is relatively little change in the partitioning after one week. Therefore, a 10 day equilibration period was selected for all other experiments. It was desirable to keep the time as short as possible to minimize any possible degradation of the HA. This experiment also verified that 1×10^{-5} M EDTA is sufficient to allow both Pu-EDTA and Pu-HA complexes to be present. This effectively allows for relatively high concentrations of Pu to be present in all fractions and puts all samples well above analytical detection limits.

The fraction of Pu-HA and Th-HA complexes in systems containing low actinide concentrations (4.3×10^{-8} M Pu and 4.9×10^{-8} M Th) are shown in Figure 4. The complexation of both Th and Pu with HA appears to increase with increasing pH. This is consistent with the relatively strong binding of Pu with deprotonation of HA. However, it is noteworthy that since EDTA is present, these data only demonstrate a change in affinity between EDTA and HA compelexes. Furthermore, the increase is modest, going from 0.70 to 0.82 in the Pu system and 0.76 to 0.93 in the Th system with increasing pH. As will be shown in the modeling discussion below,

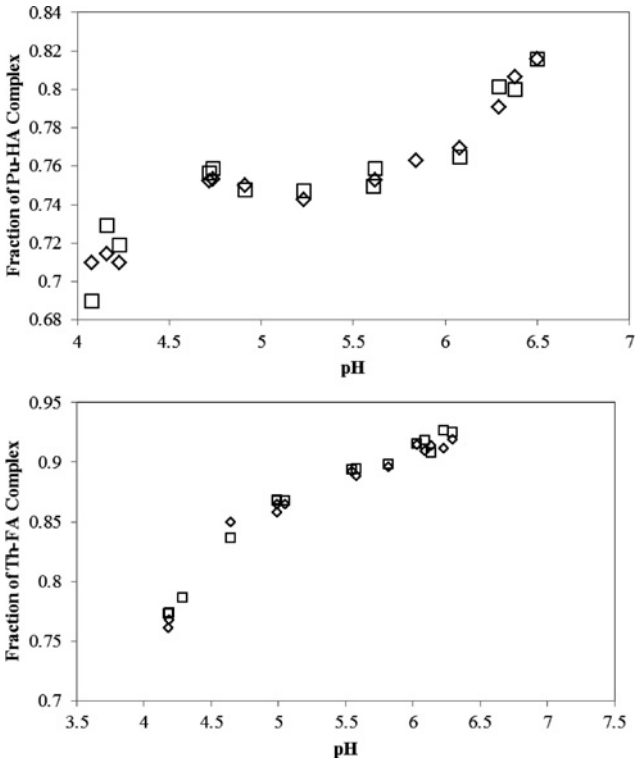


Fig. 4: Fraction of Pu (top) and Th (bottom) bound to HA as a function of pH after 10 d. System parameters: 4.3×10^{-8} M Pu, 4.9×10^{-8} M Th, 0.1 M NaCl, 10 mg C/L. Different datapoint shapes indicate duplicate aliquots taken from the same sample suspension to verify the reproducibility of the sampling scheme.

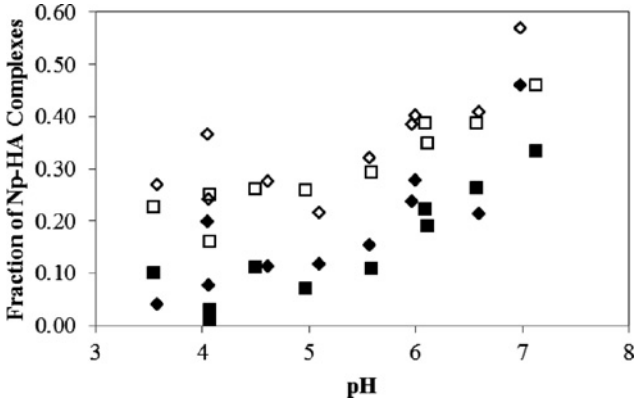


Fig. 5: Fraction of Np-HA complexes *vs.* time and pH. System parameters: 0.1 M NaCl, 10 mg C/L, 2.1×10^{-8} M Np (diamonds) or 4.2×10^{-8} M Np (squares), 24 h equilibration (closed symbols) and 14 day equilibration (open symbols).

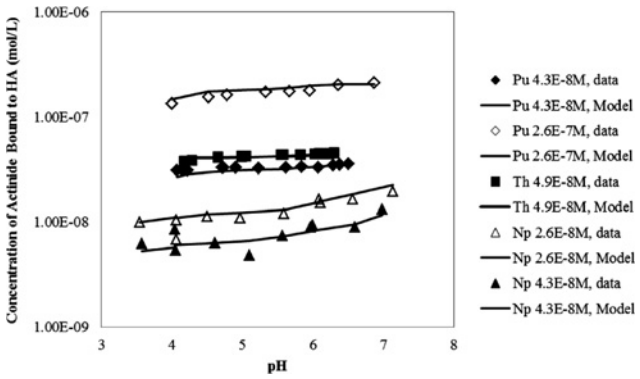


Fig. 6: Concentration of actinides bound to HA with model fits assuming discrete pKa site binding. Reactions and stability constants used in fits are provided in Table 1. All systems contained 0.1 M NaCl and 10 mg C/L HA. Diamonds represent Pu at 4.3×10^{-8} M (closed symbols) and 2.6×10^{-7} M (open symbols). Squares represent Th at 4.9×10^{-8} M. Triangles represent Np at 2.1×10^{-8} M Np (closed symbols) or 4.2×10^{-8} M Np (open symbols).

the weak influence of pH is likely a result of the exhange between EDTA and HA and the larger fraction of Th-HA complexation relative to Pu-HA is actually a result of the weaker Th-EDTA complexation relative to Pu-EDTA complexation.

Comparing the experiments with different Pu concentrations but similar HA concentrations a decrease in the fraction of Pu-HA complexes with increasing Pu concentration was observed (Figs. 3 and 4A). This is consistent with maintaining one reactant constant (HA) and increasing another (Pu) but may also represent site loading effects as the higher Pu concentration can reach 0.25% site saturation (i.e. system contains 2.6×10^{-7} M Pu relative to the HA site concentration of 1.06×10^{-4} $moles_{sites}$ L^{-1}) calculated from the HA titration data.

Complexation of Np(V) with HA increased with increasing pH (Figure 5). Furthermore, the fraction of Np bound to HA was relatively low compared with Pu(IV). This is consistent with the expected stronger complexation of tetravalent actinides as compared with pentavalent actinides. There was a slight increase in the fraction of Np-HA complexes with increasing time from 1 to 14 d. This could be interpreted as either slow complexation kinetics for the Np(V) ions or reduction of Np(V) to Np(IV), which would form stronger complexes. These data are insufficient to distinguish between slow complexation and reduction. However, previous studies which have demonstrated Np(V) reduction by HA have typically been performed under anoxic conditions and/or used a HA derivative with increased hydroquinone content [21, 22]. Furthermore, Sachs *et al.*, [23] have verified stable Np(V)-HA complexes exist using NIR spectroscopy. Therefore, given the oxic conditions of these experiments, it is assumed that minimal reduction took place for modeling purposes (discussed below).

Table 2: Reactions and stability constants describing actinide binding by HA. Uncertainty calculated by FITEQL is reported in parentheses.

Reaction	Stability Constant
$Pu^{4+} + HL3 + 2H_2O \leftrightarrow Pu(OH)_2L3^+ + 3H^+$	log K = 6.76 (0.28)
$Th^{4+} + HL3 + 2H_2O \leftrightarrow Th(OH)_2L3^+ + 3H^+$	log K = 3.58 (0.08)
$NpO_2^+ + HL1 <=> NpO_2L1 + H^+$	log K = 0.95 (0.08)
$NpO_2^+ + HL2 <=> NpO_2L2 + H^+$	log K = −1.51 (0.50)
$NpO_2^+ + HL3 <=> NpO_2L3 + H^+$	log K = −2.13 (0.07)

Actinide binding to HA was modeled using the discrete pK_a site model discussed above. Hydrolysis constants for Th(IV) and Pu(IV), EDTA protonation constants, and Pu-EDTA and Th-EDTA complexation constants were taken from available literature and databases [24–26]. A list of these constants is provided in the appendix. All constants were adjusted to 0.1 M ionic strength using the Davies equation. The model fits to the observed data are shown in Figure 6 and the reactions used to model the data are listed in Table 2. The reported error are those provided by FITEQL after assuming 5% relative error in the Pu measurements and a standard 2.3% relative error in the pH measurements. The 5% relative error in the Pu measurments is assumed as a conservative approach and is significantly higher than replicate ICPMS measurements (generally < 1% deviation). The more conservative value of 5% was used due to the indirect nature of the ultrafiltration/ligand competition experimental approach used in this work.

Overall, the model provides an acceptable fit to the data. Initial attempts to model the Th(IV) and Pu(IV) datasets without assuming a partially hydrolyzed species using the reaction:

$$An^{4+} + HL \leftrightarrow AnL^{3+} + H^{+} \quad (5)$$

could not capture the pH dependence of the data and would drastically under-predict Pu-HA and Th-HA binding at higher pH values. Interestingly reactions using unhydrolyzed Pu as shown in Eq. (5) were able to fit Pu(IV) binding to citric acid, alginic acid, and extracellular polymeric substances using 1 : 1, 1 : 2, and 1 : 3 Pu : ligand complexes ([16, 17]). However, it is noteworthy that these constants were determined only at pH 4 where the ligands may successfully compete with hydrolysis. In order to describe the Pu-HA complexation observed in this work, inclusion of partially hydrolyzed species based on the generalized reaction:

$$An^{4+} + (4-x)H_2O + yHL \leftrightarrow An(OH)_{(4-x)}L_y + (4+y-x)H^{+} \quad (6)$$

was necessary. Attempts were made to model the data using all possible iterations of reactions 5 and 6 with x ranging from 0 to 4 and y ranging from 1 to 3 and the reactions shown in Table 2 provide the best fit to the data as determined by the weighted sum of squares/difference of fit values in FITEQL. The Pu(IV)-HA complexation constant of 6.76 (0.28) using data from experiments with Pu at two concentrations. When fitting the datasets individually, stability constants of 6.62 and 6.84 are found for the high and low concentration datasets, respectively. This variation is within the uncertainty of the value determined using both datasets simultaneously. Furthermore, since the conditional Pu-HA stability constant was determined *via* competition reactions with EDTA, it is important to note the influence of the Pu-EDTA stability constants on the resulting Pu-HA constant. The uncertainty associated with Pu-EDTA complexation is not accounted for in the FITEQL model and therefore the reported uncertianty in the Pu-HA complexation constant is underestimated. Similar to the modeling effort described in this work, where the inclusion of a hydrolyzed species was essential for accurately predicting experimental data, species such as $[Pu(EDTA)(OH)]^{-}$ and $[Pu(EDTA)(OH)_2]^{2-}$ play a dominant role in systems containing both Pu and EDTA; yet are not well understood ([25, 27]). Therefore, every effort must be made to utilize the best available constants for studies of this nature, as these constants represent a potential source of error.

When examining Pu(IV)-EDTA complexation, Boukhalfa *et al.* [25] included the species $[Pu(EDTA)_2H_3]^{-}$ while Meyer *et al.* [27] included $[Pu(EDTA)_2H_2]^{2-}$. Meyer *et al.* [27] used an iterative process of excluding data points, based on the theoretical solubility of $Pu(OH)_4(am)$, which resulted in a truncated dataset (deemed insufficient for inclusion in this study). However, for comparison purposes, the Meyer *et al.* [27] Pu-EDTA stability constants were used to model the global Pu data. The resulting Pu-HA stability constant (HL3 basis) of 6.72 is in good agreement with the value of $\log \beta = 6.76 \pm 0.14$ calculated based on the Pu-EDTA stability constants from Boukhalfa *et al.* [25].

Given the considerations above, under the experimental conditions in this work, the dominant EDTA and Pu-EDTA species are H_2EDTA^{2-}, $HEDTA^{3-}$, $Pu(EDTA)H^{3+}$ and $Pu(EDTA)(OH)^{-}$. Combining these reactions with the Pu-HA complexation reaction in Table 2 can yield the following equations all of which have either no influence of pH or a weaker influence of pH relative to the Pu-HA complexaiton reaction in Table 2. Despite showing the Pu-HA complexation as a reaction with Pu^{4+} in Table 2. These reactions are actually what is occuring during the experiments and help to explain the weak influence of pH in Figs. 3 and 4. Note these reactions are written for the HL3 ($pK_a = 7$) humic acid site with EDTA-4 represented as Y.

$$PuY_2H^{3-} + HL3 + 2H_2O(2YH_2^{2-} + Pu(OH)_2L3^{+}$$
$$PuY_2H^{3-} + HL3 + 2H_2O(2YH^{3-} + Pu(OH)_2L3^{+} + 2H^{+}$$
$$PuY(OH)^{-} + HL3 + H_2O(YH^{3-} + Pu(OH)_2L3^{+} + H^{+}$$
$$PuY(OH)^{-} + HL3 + H_2O(YH_2^{2-} + Pu(OH)_2L3^{+}$$

As discussed previously, Banik *et al.* [3] and Buda *et al.*, [9] reported conditional stability constants of 6.4–8.4 over the pH range 1.8 to 4 using a charge neutralization model. The model is based on the expression

$$\beta = \frac{[MHA(z)]}{[M^{z+}] \cdot ([HA(z)]_t \cdot LC - [MHA(z)])} \quad (7)$$

where [MHA(z)] is the metal-HA complex for a metal of charge z, $[M^{z+}]$ is the free metal concentration, $[HA(z)]_t$ is the total concentration of humic acid, and LC is a loading capacity term. The loading capacity is defined as:

$$LC = \frac{[MHA(z)]}{[HA(z)]_t} = \frac{z \cdot [M^{z+}]}{PEC \cdot (HA)} \quad (8)$$

where PEC is the proton exchange capacity of the humic acid and (HA) is the mass concentration of humic acid in the suspension. Due to differences in the conceptual model used to describe proton-binding by the HA, and calculate the resulting binding site concentrations (discrete pK_a spectrum (this work) *vs.* normalization to a loading capacity term ([3, 9]), the Pu-HA stability constant determined in this work cannot be directly compared with the

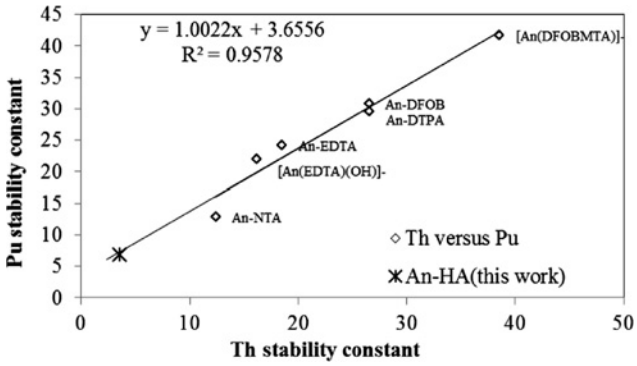


Fig. 7: Plot of Th-ligand stability constants *vs.* the corresponding Pu-ligand constants.

literature values. It is noteworthy that Banik *et al.*, [3] and Buda *et al.*, [9] also reported Pu complexation with HA as the $Pu(OH)_2^{2+}$-HA species, similar to the $Pu(OH)_2L$ species found in this work. In an attempt to compare the literature data to the current work, the ratios of HA-bound Pu to free-Pu were calcuated using the PEC, LC, and log β values reported by Banik *et al.*, [3] and Buda *et al.*, [9] in a 10 mg/L HA solution. The log ratios at pH 3 and 4 are 6.16 and 6.52, respectively. When calcuating the same ratio using the Pu-HA complexation constant reported in this work, which also considers HA speciation *via* pK_a values and Pu hydrolysis, ratios of 5.47 and 5.50 were calcualted for pH 3 and 4, respectively. This is considered acceptable agreement given the differences in the experimental and theoretical methods involved.

Reiller *et al.* [28] calculated Th-HA log β values of 16.2, 17.3, and 19.3 at pH 6.75, 7.2, and 7.9, respectively, using competition sorption studies with silica. These stability constants are based on the equation:

$$\beta = \frac{[\text{Th HA}]}{[\text{Th}][\text{HA}]} \quad (9)$$

Where [HA] is a molar concentration of HA based on the exchange site concentration. This model does not consider any changes in HA speciation *vs.* pH. Thus, the influence of pH noted above is likely due to changes in Th speciation and competition with silica sorption. Due to this, differences in the conceptual model used to describe metal- and proton-binding by the HA preclude comparison beyond simply stating that Reiller *et al.* (2003) [28] found the Th-HA complex to be favorable, which is consistent with the findings of this study.

An interesting observation in this work is that the Pu-HA complexation constant is approximately 3 orders of magnitude greater than the Th-HA complexation constant. Given the common use of Th(IV) as a chemical analog for Pu(IV), it is expected that the constants would be much more similar. However, including the An(IV)-HA stability constants in a plot with other large organic ligands (Figure 7), it can be seen that 1) there is excellent agreement between the Pu(IV)-HA and Th(IV)-HA stability constants determined as part of this work (shown as the x in Figure 7) and values for Th(IV) and Pu(IV) complexation with other organic ligands and 2) the intercept of the regression line is 3.7. This positive intercept verifies the stronger complexation of Pu(IV) relative to Th(IV) for the same ligands. This demonstrates the importance of performing studies using Pu(IV) rather than Th(IV) as an analog.

Three reactions were required in order to accurately model the complexation of Np(V) with HA. As discussed above, the data were modeled assuming only Np(V) was present. There is a large amount of scatter in the data due to the relatively weak Np(V)-HA complexes (Figure 6). The "free" concentration of Np was modeled in order to have greater certainty in the analytical measurements. This in effect caused scatter in the data when plotted as "fraction Np-HA" as shown in Figure 6 due to subtraction of a two relatively large numbers from each other. The model accurately predicts the observed free Np concentration (data not shown). The three sites (HL1, HL2, and HL3) were necessary to capture the pH dependence of the complexation reaction. This is due to the relatively weak complexation and much stronger influence of pH, as compared with Pu(IV). Consistent with the expected weaker binding of Np(V) relative to Pu(IV), the Np(V)-HA complexation constants are several orders of magnitude lower than Pu(IV)-HA constants. This provides circumstantial evidence that no reduction of Np(V) to Np(IV) occurred in these studies.

The majority of experiments examining Np-NOM complexation to date have utilized the charge neutralization model. Therefore, direct comparisons of the calculated stability constants cannot be made. However, the general trend of increasing Np(V)-HA complexation with increasing pH was observed in this work as well as several other researchers ([29–33]. Seibert *et al.*, [29] utilized the charge neutralization model and determined stability constants of 5.0 ± 0.3 at total Np(V) concentrations of 10^{-11} mol/L and observed a continuous decrease of the stability constant to 3.7 ± 0.4 as the Np(V) concentration increased from 10^{-7} to 5.0×10^{-4} mol/L. Additional stability constants of 3.53 ± 0.04 and 3.53 ± 0.05 were determined for Np(V)-FA and Np(V)-HA complexation, respectively, using the charge neutralization model [30–32]. The data of Shcherbina *et al.*, [33] provide the most direct comparison with literature values as Np(V) complexation with Leonardite HA was examined, among several other HA derivatives. A conditional binding constant of 2.26 ± 0.16

was determined at pH 4.7 using the expression:

$$\beta = \frac{[NpO_2{}^+HA]}{[NpO_2{}^+]_{free}[HA]_{free}} \quad (10)$$

where $[NpO_2{}^+HA]$ is the concentration of Np(V)-HA complexes, $[NpO_2{}^+]_{free}$ is the free concentration of neptunium, and $[HA]_{free}$ is the concentration of proton exchange sites on the HA. Shcherbina *et al.*, [33], made the assumption that $[HA]_{free}$ is equal to the total concentration of proton exchange sites given the large excess of HA relative to Np thus giving the stability constant units of L mol^{-1}. Recalculating the stability constants from the current dataset based on this modeling approach yields a series of relatively consistent stability constants with increasing pH where the average value is $\log \beta = 3.85$ with a standard deviation of 0.07. This value is significantly higher than the value determined by Shcherbina *et al.*, [33]. However, as discussed above for the stability constants determined by Seibert *et al.*, [29], as the Np concentration increased, there was an observed decrease in the Np(V)-HA stability constant. A similar phenomena is likely occurring here where a higher value of 3.85 has been observed for experiments with $\sim 10^{-8}$ M Np(V) as compared with experiments with $\sim 10^{-5}$ M Np(V) in the study by Shcherbina et al., [33].

3.3 Ternary sorption experimental and modeling studies

The sorption of Pu(IV) and Pu(V) to gibbsite after 7 d is shown in Figure 8. There is relatively little change in the sorption behavior as a function of time between 1 and 7 d (data not shown). Previous sorption experiments indicated that changes in the sorption behavior were continuously observed over a 60 day period and were attributed to reduction of Pu(V) to Pu(IV) [34]. Similar surface mediated reduction of Pu(V) has been observed on a variety of pure minerals and soils [35–41] and sorption of Pu(IV) is considerably stronger than Pu(V). A double layer surface complexation model fit to the data is shown as the solid lines in Figure 8 and the aqueous and surface complexation constants are given in Table 3.

Sorption isotherms examining Pu(IV) sorption to gibbsite at pH 4 and 6 in the presence of 10 mg/L Leonardite humic acid (LHA) are shown in Figure 9. The scales in the top and bottom plots in Figure 9 are intentionally the same to allow comparison. The pH 6 dataset exhibited less sorption than the pH 4 dataset. In binary systems containing only Pu and gibbsite, this result would be unexpected based on frequent observations of increasing sorption with increasing pH (as shown in Figure 8). To verify this, the surface complexation model based on the Pu(IV) and Pu(V) sorption edges shown above was used to predict the sorption assuming no influence of the HA. This model is represented by the solid black lines in Figure 9. It can be seen that the model accurately predicts greater sorption at pH 6 relative to pH 4. However, when Pu-HA complexation is incorporated into the calucations using the stability constant in Table 2, the model results are significantly different. When assuming no sorption of the HA or Pu-HA complexes, the majority of Pu is assumed to be present as an aqueous $Pu(OH)_2L3^+$ complex and the sorbed concentration is under-predicted by over an order of magnitude (model output not shown). This observation implies that a ternary gibbsite-Pu-HA complex may be influencing these data. Such a complex could explain the greater sorption of Pu observed at pH 4 as compared with pH 6 due to sorption of the ligand to the surface which in turn carries Pu(IV). These would be Type B sorption complexes, as proposed by Schindler [43] and is consistent with the expected sorption of HA at low pH . This behavior could be described with a ternary surface complexation model. However, while this type of modeling effort is useful for providing quantitative predictions of the aqueous and sorbed concentrations, it is important to note that this model is purely a fitting exercise and that the existence of surface complexes such as the ternary complex must be spectroscopically verified. However, it is clear that the presence of HA can alter the extent of sorption of Pu to gibbsite. In the case of the pH 4 system, HA causes an increase in sorption relative to the HA free system while at pH 6, the HA causes a slight decrease in sorption relative to the HA free system. The increased sorption of metals at low pH values which is apparently facilitated by humic acid

Table 3: Aqueous and surface complexation constants used to model Pu-HA-gibbsite system.

Reaction	log K
$Pu^{4+} + H_2O \leftrightarrow PuOH^{3+} + H^+$	0.6[a] (−0.04)[c]
$Pu^{4+} + 2H_2O \leftrightarrow Pu(OH)_2^{2+} + 2H^+$	0.6[a] (−0.47)[c]
$Pu^{4+} + 3H_2O \leftrightarrow Pu(OH)_3^{+} + 3H^+$	−2.3[a] (−3.58)[c]
$Pu^{4+} + 4H_2O \leftrightarrow Pu(OH)_4^{0} + 4H^+$	−8.5[a] (−9.78)[c]
$\equiv AlOH \leftrightarrow \equiv AlO^- + H^+$	8.33[b]
$\equiv AlOH + H^+ \leftrightarrow \equiv AlOH_2^+$	−9.73[b]
$Pu^{4+} + \equiv AlOH + H_2O <=> \equiv AlOPu(OH)^{++} + 2H^+$	14.81
$Pu^{4+} + \equiv AlOH + 2H_2O <=> \equiv AlOPu(OH)_2^{+} + 3H^+$	5.36
$Pu^{4+} + \equiv AlOH + 3H_2O <=> \equiv AlOPu(OH)_3^{o} + 4H^+$	−3.55
$PuO_2^+ + \equiv AlOH <=> \equiv AlOPuO_2 + H^+$	−1.93

[a] [24]
[b] [42]
[c] Values corrected to 0.1 M NaCl using the Davies equation

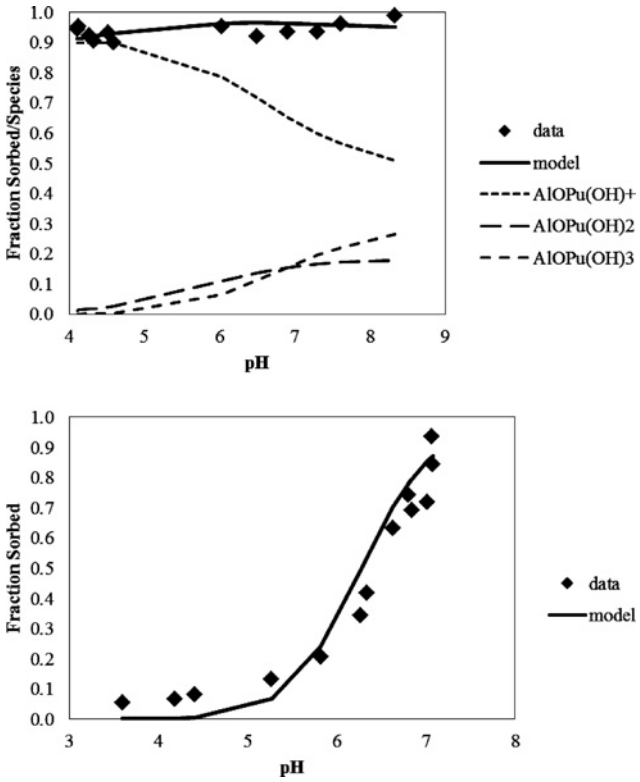


Fig. 8: Sorption of Pu(IV) (top) and Pu(V) (bottom) to gibbsite *vs.* pH. The solid black line indicates the surface complexation model fit using the constants listed in Table 3. Individual species from the Pu(IV)-gibbsite systems are represented by dashed black lines. The Pu(V) system utilized only on surface complex, thus no dashed line is shown. System parameters: $[Pu]_{total} = 1.1 \times 10^{-10}$ mol/L, [NaCl] = 10 mM, [gibbsite] = 5 g/L, atmospheric conditions.

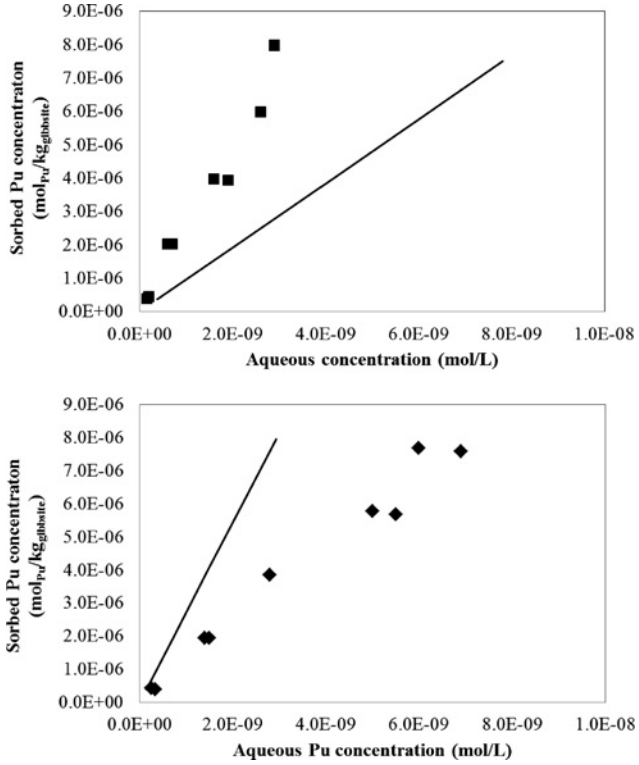


Fig. 9: Influence of Leonardite humic acid on Pu(IV) sorption to gibbsite under oxic conditions at pH 4 (top) and pH 6 (bottom). Data points represent Pu concentrations measured when separating the solid/aqueous phases using centrifugation to eliminate particles less than 100 nm from suspension. Thus aqueous Pu-HA complexes should remain in solution. Solid line represents surface complexation model predicting sorption in the absence of HA. System conditions: [HA] = 10 mg C/L, [gibbsite] = 10 g/L, [Pu] = variable, [NaCl] = 0.1 M.

has even been recently proposed as a method for remediation of contaminated sites [44]. This a remarkable shift in the conceptual model that the presence of organic ligands will increase the mobility of the actinides.

4 Conclusions

The over-arching purpose of this research has been to examine the influence of HA on Pu geochemical behavior through a series of laboratory studies. While the system conditions have been simplified relative to environmental conditions (e.g., purified gibbsite was used in lieu of natural soil suspensions), this data will serve to inform future studies under more environmentally relevant conditions. The conditional stability constant for the Pu-HA complex of 6.76±0.14 was determined over the pH range 4-7 using a hybrid ultra-filtration/equilibrium dialysis ligand exchange approach. This value is three orders of magnitude higher than the Th(IV)-HA constant and between six and eight orders of magnitude higher than the Np(V)-HA complexes. The magnitude of the stability constants and the general trend of increasing complexation strength with increasing pH is consistent with previous observations. Another important finding during the complexation studies, involved the influence of titration hysteresis on the final Pu-HA stability constant. While every effort should be made to conduct titrations in a fashion that is consistent with the current body of knowledge surrounding proton-binding by HAs, the amount of error that is present in studies of this nature (assumed to be 5% in this work) makes the contribution from titration hysteresis appear minimal.

Finally, sorption experiments with and without HA present were performed and the results were modeled using a double layer surface complexation model. The data show increased sorption of Pu in the presence of HA as well as greater sorption at pH 4 relative to pH 6, which would not be expected in the absence of HA. Therefore, this study demonstrates that ternary Pu-HA-gibbsite com-

plexes may form under lower pH conditions and exhibit greater sorption than that observed in the absence of HA. This finding indicates that although the presence of HA may increase the solubility/aqueous concentrations of Pu in the absence of a solid phase, formation of ternary complexes may indeed retard the subsurface migration of Pu. The corollary to this finding is that the sorbent involved in the ternary complex is part of the subsurface matrix rather than a mobile colloid. In the case where a mobile colloid is involved, the ternary complexes may indeed stabilize sorbed Pu on mobile colloids and allow for enhanced transport. The influence of HA on Pu in more realistic representations of environmental systems must be examined before definitive conclusions can be drawn. Furture experiments will focus on different types of NOM and different solid phases.

Appendix

Table 4: Stability constants for Humic acid, EDTA, and hydrolysis used in determination of actinide-HA stability constants. Note $Y^{4-} = EDTA^{4-}$.

Reaction	Value
$HL1 \leftrightarrow H^+ + L1^-$	$pK_a = 3$
$HL2 \leftrightarrow H^+ + L2^-$	$pK_a = 5$
$HL3 \leftrightarrow H^+ + L3^-$	$pK_a = 7$
$HL4 \leftrightarrow H^+ + L4^-$	$pK_a = 9$
$Pu^{4+} + H_2O \leftrightarrow Pu(OH)^{3+} + H^+$	-0.04[a]
$Pu^{4+} + 2H_2O \leftrightarrow Pu(OH)_2^{2+} + 2H^+$	-0.47[a]
$Pu^{4+} + 3H_2O \leftrightarrow Pu(OH)_3^{+} + 3H^+$	-3.58[a]
$Pu^{4+} + 4H_2O \leftrightarrow Pu(OH)_4(aq) + 4H^+$	-9.78[a]
$Y^{4-} + H^+ \leftrightarrow YH^{3-}$	9.52[b]
$Y_H^{3-} + H^+ \leftrightarrow YH_2^{2-}$	6.13[b]
$YH_2^{2-} + H^+ \leftrightarrow YH_3^{-}$	2.69[b]
$YH_3^{-} + H^+ \leftrightarrow YH_4^{0}$	2[b]
$YH_4^{0} + H^+ \leftrightarrow YH_5^{+}$	1.5[b]
$YH_5^{+} + H^+ \leftrightarrow YH_6^{2+}$	0b
$Pu^{4+} + Y^{4-} \leftrightarrow PuY(aq)$	24.2[b]
$Pu^{4+} + Y^{4-} + H_2O \leftrightarrow [PuY(OH)]^- + H^+$	21.95[b]
$Pu^{4+} + Y^{4-} + 2H_2O \leftrightarrow [PuY(OH)_2]^{2-} + 2H^+$	15.29[b]
$Pu^{4+} + 2Y^{4-} \leftrightarrow [Pu(Y)_2]^{4-}$	35.39[b]
$Pu^{4+} + 2Y^{4-} + H^+ \leftrightarrow [Pu(Y)_2H]^{3-}$	42.75[b]
$Pu^{4+} + 2Y^{4-} + 3H^+ \leftrightarrow [Pu(Y)_2H_3]^{-}$	47.39[b]
$Th^{4+} + H_2O \leftrightarrow Th(OH)^{3+} + H^+$	-2.84[a]
$Th^{4+} + 2H_2O \leftrightarrow Th(OH)_2^{2+} + 2H^+$	-7.07[a]
$Th^{4+} + 3H_2O \leftrightarrow Th(OH)_3^{+} + 3H^+$	-12.28[a]
$Th^{4+} + 4H_2O \leftrightarrow Th(OH)_4(aq) + 4H^+$	-18.78[a]
$Th^{4+} + Y^{4-} \leftrightarrow ThY(aq)$	23.2[c]
$Th^{4+} + Y^{4-} + H^+ \leftrightarrow [ThYH]^+$	25.2[c]
$Th^{4+} + Y^{4-} + H_2O \leftrightarrow [ThY(OH)]^- + H^+$	16.16[c]
$2Th^{4+} + 2Y^{4-} + 2H_2O \leftrightarrow [Th_2(Y)_2(OH)_2]^{2-} + 2H^+$	36.58[c]

[a] Neck and Kim, 2001
[b] Boukhalfa *et al.* 2004
[c] NIST Standard Reference Database 6 Version 7

Acknowledgement: The authors wish to thank Dr. Annie B. Kersting of Lawrence Livermore National Laboratory and Dr. Ruth Tinnacher of Lawrence Berkeley National Laboratory for helpful discussions regarding this work. This work was supported by the Subsurface Biogeochemical Research Program of the U. S. Department of Energy's Office of Biological and Environmental Research.

Received January 5, 2013; accepted December 30, 2013.

References

1. Doucet, F. J., Lead, J. R., Santschi, P. H.: Colloid-trace element interactions in aquatic systems, in Environmental Colloids and Particles: Behavior, Separation, and Characterization, Wilkinson, K. J., Lead, J. R. (Eds.), John Wiley & Sons, West Sussex, England 2007, p. 95.
2. Andre, C., Choppin, G. R.: Reduction of Pu(V) by humic acid. Radiochimica Acta 88, 613 (2000).
3. Banik, N. L., Buda, R. A., Burger, S., Kratz, J. V., Trautmann, N.: Speciation and interactions of plutonium with humic substances and kaolinite in aquifer systems. Journal of Alloys and Compounds 444, 522 (2007).
4. Bao, H. M., Michalski, G. M., Thiemens, M. H.: Sulfate oxygen-17 anomalies in desert varnishes. Geochimica et Cosmochimica Acta 65, 2029 (2001).
5. Marquardt, C. M., Seibert, A., Artinger, R., Denecke, M. A., Kuczewski, B., Schild, D., Fanghanel, T.: The redox behaviour of plutonium in humic rich groundwater. Radiochimica Acta 92, 617 (2004).
6. Roberts, K. A., Santschi, P. H., Honeyman, B. D.: Pu(V) reduction and enhancement of particle-water partitioning by exopolymeric substances. Radiochimica Acta 96, 739 (2008).
7. Blinova, O., Novikov, A., Perminova, I., Goryachenkova, T., Haire, R.: Redox interactions of Pu(V) in solutions containing different humic substances. Journal of Alloys and Compounds 444, 486 (2007).
8. Banik, N. L., Buda, R. A., Burger, S., Kratz, J. V., Trautmann, N.: Sorption of tetravalent plutonium and humic substances onto kaolinite. Radiochimica Acta 95, 569 (2007).

9. Buda, R. A., Banik, N. L., Kratz, J. V., Trautmann, N.: Studies of the ternary systems humic substances - kaolinite - Pu(III) and Pu(IV). Radiochimica Acta 96, 657 (2008).
10. Liu, C. L., Yang, Y. E., Wang, Z. M., Li, S. S., Guo, Z. D., Li, B., Jiang, L., Jiang, H., Wang, L., Li, D., Du, Z. D.: Influence of humic substances on the migration of Np-237, Pu-238 and Am-241 in a weak loess aquifer. Radiochimica Acta 89, 387 (2001).
11. Nelson, D. M., Penrose, W. R., Karttunen, J. O., Mehlhaff, P.: Effects of dissolved organic carbon on the adsorption properties of plutonium in natural waters. Environ. Sci. Technol. 19, 127 (1985).
12. Righetto, L., Bidoglio, G., Azimonti, G., Bellobono, I. R.: Competitive actinide interactions in colloidal humic-acid mineral oxide systems. Environ. Sci. Technol. 25, 1913 (1991).
13. Powell, B. A., Rao, L. F., Nash, K. L.: Effect of 1-hydroxyethane-1,1-diphosphonic acid (HEDPA) on partitioning of Np and Pu to synthetic boehmite. Separation Science and Technology 45, 721 (2010).
14. l Kim, J. I., Czerwinski, K. R.: Complexation of metal ions with humic acid: metal ion charge neutralization model. Radiochimica Acta 73, 5 (1996).
15. Westall, J. C., Jones, J. D., Turner, G. D., Zachara, J. M.: Models for association of metal-ions with heterogeneous environmental sorbents .1. Complexation of Co(Ii) by Leonardite humic-acid as a function of Ph and Naclo4 concentration. Environ. Sci. Technol. 29, 951 (1995).
16. Harper, R. M., Kantar, C., Honeyman, B. D.: Binding of Pu(IV) to galacturonic acid and extracellular polymeric substances (EPS) from *Shewanella putrefaciens*, *Chlostridium* sp. and *Pseudomonas fluorescens*. Radiochimica Acta 96, 753 (2008).
17. Kantar, C., Honeyman, B. D.: Plutonium (IV) complexation with citric and alginic acids at low Pu(T) concentrations. Radiochimica Acta 93, 757 (2005).
18. Bryan, N. D., Abrahamsen, L., Evans, N., Warwick, P., Buckau, G., Weng, L. P., Van Riemsdijk, W. H.: The effects of humic substances on the transport of radionuclides: recent improvements in the prediction of behaviour and the understanding of mechanisms. Applied Geochemistry 27, 378 (2012).
19. Vanloon, L. R., Granacher, S., Harduf, H.: Equilibrium dialysis-ligand exchange - a novel method for determining conditional stability-constants of radionuclide-humic acid complexes. Analytica Chimica Acta 268, 235 (1992).
20. Lenhart, J. J., Honeyman, B. D.: Uranium(VI) sorption to hematite in the presence of humic acid. Geochimica et Cosmochimica Acta 63, 2891 (1999).
21. Schmeide, K., Bernhard, G.: Redox stability of neptunium(V) and neptunium(IV) in the presence of humic substances of varying functionality. Radiochimica Acta 97, 603 (2009).
22. Shcherbina, N. S., Kalmykov, S. N., Perminova, I. V., Kovalenko, A. N.: Reduction of actinides in higher oxidation states by hydroquinone-enriched humic derivatives. Journal of Alloys and Compounds 444, 518 (2007).
23. Sachs, S., Schmeide, K., Reich, T., Brendler, V., Heise, K. H., Bernhard, G.: EXAFS study on the neptunium(V) complexation by various humic acids under neutral pH conditions. Radiochimica Acta 93, 17 (2005).
24. Neck, V., Kim, J. I.: Solubility and hydrolysis of tetravalent actinides. Radiochimica Acta 89, 1 (2001).
25. Boukhalfa, H., Reilly, S. D., Smith, W. H., Neu, M. P.: EDTA and mixed-ligand complexes of tetravalent and trivalent plutonium. Inorganic Chemistry 43, 5816 (2004).
26. Martell, A. E., Smith, R. K.: Critical Stability Constants, Standard Reference Database 46, Version 6.30, National Institute of Standards, Gaithersburg, MD 2001.
27. Meyer, M., Burgat, R., Faure, S., Batifol, B., Hubinois, J. C., Chollet, H., Guilard, R.: Thermodynamic studies of actinide complexes. 1. A reappraisal of the solution equilibria between plutonium(TV) and ethylenediaminetetraacetic acid (EDTAH(4)) in nitric media. Comptes Rendus Chimie 10, 929 (2007).
28. Reiller, P., Moulin, V., Casanova, F., Dautel, C.: On the study of Th(IV)-humic acid interactions by competition sorption studies with silica and determination of global interaction constants. Radiochimica Acta 91, 513 (2003).
29. Seibert, A., Mansel, A., Marquardt, C. M., Keller, H., Kratz, J. V., Trautmann, N.: Complexation behaviour of neptunium with humic acid. Radiochimica Acta 89, 505 (2001).
30. Chen, C. C., Coleman, M. L., Katz, L. E.: Bridging the gap between macroscopic and spectroscopic studies of metal ion sorption at the oxide/water interface: Sr(II), Co(II), and Pb(II) sorption to quartz. Environ. Sci. Technol. 40, 142 (2006).
31. Marquardt, C., Kim, J. I.: Complexation of Np(V) with fulvic acid. Radiochimica Acta 81, 143 (1998).
32. Marquardt, C., Kim, J. I.: Complexation of Np(V) with humic acid: intercomparison of results from different laboratories. Radiochimica Acta 80, 129 (1998).
33. Rodda, D. P., Johnson, B. B., Wells, J. D.: Modeling the effect of temperature on adsorption of lead(II) and zinc(II) onto goethite at constant pH. Journal of Colloid and Interface Science 184, 365 (1996).
34. Powell, B. A., Kersting, A. B., Zavarin, M., Zhao, P.: Development of a Composite Non-Electrostatic Surface Complexation Model Describing Plutonium Sorption to Aluminosilicates, LLNL-TR-408276, Lawrence Livermore National Laboratory, Livermore, California 2008.
35. Hixon, A. E., Hu, Y. J., Kaplan, D. I., Kukkadapu, R. K., Nitsche, H., Qafoku, O., Powell, B. A.: Influence of iron redox transformations on plutonium sorption to sediments. Radiochimica Acta 98, 685 (2010).
36. Powell, B. A., Fjeld, R. A., Kaplan, D. I., Coates, J. T., Serkiz, S. M.: Pu(V)O2+ adsorption and reduction by synthetic hematite and goethite. Environ. Sci. Technol. 39, 2107 (2005).
37. Kalmykov, S. N., Kriventsov, V. V., Teterin, Y. A., Novikov, A. P.: Plutonium and neptunium speciation bound to hydrous ferric oxide colloids. Comptes Rendus Chimie 10, 1060 (2007).
38. Romanchuk, A. Y., Kalmykov, S. N., Aliev, R. A.: Plutonium sorption onto hematite colloids at femto- and nanomolar concentrations. Radiochimica Acta 99, 137 (2011).
39. Powell, B. A., Duff, M. C., Kaplan, D. I., Fjeld, R. A., Newville, M., Hunter, D. B., Bertsch, P. M., Coates, J. T., Eng, P., Rivers, M. L., Serkiz, S. M., Sutton, S. R., Triay, I. R., Vaniman, D. T.: Plutonium oxidation and subsequent reduction by Mn(IV) minerals in Yucca Mountain tuff. Environ. Sci. Technol. 40, 3508 (2006).
40. Sanchez, A. L., Murray, J. W., Sibley, T. H.: The adsorption of plutonium-IV and plutonium-V on goethite. Geochimica et Cosmochimica Acta 49, 2297 (1985).
41. Keeney-Kennicutt, W. L., Morse, J. W.: The redox chemistry of Pu(V)O2+ interaction with common mineral surfaces in dilute

solutions and seawater. Geochimica et Cosmochimica Acta 49, 2577 (1985).
42. Turner, D. R.: A uniform approach to surface complexation modeling of radionuclide sorption, Center for Nuclear Waste Regulatory Analyses, San Antonio 1995, p. 103.
43. Schindler, P. W.: Co-adsorption of metal ions and organic ligands: formation of ternary surface complexes, in Mineral-Water Interface Geochemistry, Hochella Jr., M. F., White, A. F. (Eds.), Mineralogical Society of America, Washington, DC 1990, p. 281.
44. Wan, J. M., Dong, W. M., Tokunaga, T. K.: Method to attenuate U(VI) mobility in acidic waste plumes using humic acids. Environ. Sci. Technol. 45, 2331 (2011).